LA-UR- 96-2390

CONF-9609241--2

Title: REGIONAL SEISMIC DISCRIMINATION IN CENTRAL ASIA WITH EMPHASIS ON WESTERN CHINA



Author(s): HANS E. HARTSE, GEOPHYSICS GROUP EES-3, MS C335, LOS ALAMOS NATIONAL LABORATORY

STEVEN R. TAYLOR, GEOPHYSICS GROUP EES-3, MS C335, LOS ALAMOS NATIONAL LABORATORY

WILLIAM S. PHILLIPS, GEOPHYSICS GROUP EES-3, MS C335, LOS ALAMOS NATIONAL LABORATORY

GEORGE E. RANDALL, GEOPHYSICS GROUP EES-3, MS C335, LOS ALAMOS NATIONAL LABORATORY

Submitted to: PROCEEDINGS OF THE 18TH ANNUAL SEISMIC RESEARCH SYMPOSIUM SPONSORED BY PHILLIPS LABORATORY



Los Alamos
NATIONAL LABORATORY



Form No. 836 R5
ST 2629 10/91

# Regional Seismic Discrimination in Central Asia With Emphasis on Western China

Hans E. Hartse, Steven R. Taylor, W. Scott Phillips, and George E. Randall
*Geophysics Group - EES-3, Los Alamos National Lab*

Sponsored by U.S. Department of Energy, Contract W-7405-ENG-36
Comprehensive Test Ban Treaty Research and Development Program, ST482A

## ABSTRACT

In support of an anticipated Comprehensive Test Ban Treaty, we have started to evaluate regional seismic event discrimination capabilities for central Asia, emphasizing western China. We have measured noise and seismic phase amplitudes of over 250 earthquakes and 18 underground nuclear explosions recorded at the broadband, digital station WMQ in western China and over 100 earthquakes and 5 nuclear explosions at station AAK in Kyrgyzstan. The explosions are from the Kazakh Test Site (KTS) and Lop Nor, China. The earthquakes are mostly from northwest China. We have also evaluated a single suspected chemical explosion. Event magnitudes ($m_b$) range between 2.5 and 6.5 and maximum event-station distance is about 1700 km. Using these measurements we formed phase, spectral, cross-spectral, short-period/long-period, and long-period ratios to test many possible event discriminants. All ratios were corrected for distance effects before forming ratio-versus-magnitude discrimination plots.

The most consistent discriminants for separating earthquakes from explosions are a high-frequency ($f > 4\,Hz$) $P/S$ ratio versus $m_b$ and a short-period $P$ ($f > 1\,Hz$) - to - long-period Rayleigh-wave ($0.05\,Hz < f < 0.1\,Hz$) ratio versus $m_b$. For the short-period $P/S$ ratio, separation between earthquakes and explosions increases as frequency increases. $P_n$, $P_g$, and $S_n$ spectral ratios (3–6 $Hz$ / 0.75–1.5 $Hz$) and $P$ (3–6 $Hz$) / $S$ (0.75–1.5 $Hz$) cross-spectral ratios also separate most earthquakes from the explosions. In contrast to the western United States, the $L_g$ spectral ratio does not separate the events in central Asia. We believe this observation is related to the source effects of hard-rock geology and a near-surface water table for the Asian test sites. $P$ spectral ratios may prove to be useful discriminants in cases where path effects block $L_g$ propagation, making the $P_g/L_g$ ratio unavailable. The cross-spectral ratios, involving high-frequency $P$ and low-frequency $L_g$, may also prove useful as smaller explosions recorded at greater distances can be evaluated compared to the high-frequency $P/L_g$ ratio. The KTS explosions separate from earthquakes when an $R/L$ (Rayleigh-wave/Love-wave) ratio is formed. The large Lop Nor explosions do not separate from the earthquakes when the $R/L$ ratio is formed, possibly indicating strong tectonic release is associated with explosions at the Lop Nor test site. However, because we have examined only one path at a single station for these explosions, source-radiation pattern may be influencing this observation. For station AAK, the short-period spectral and cross-spectral ratios identify a few earthquakes (not recorded at WMQ) from the north Pamir region that plot with the Lop Nor explosions. The waveforms from these earthquakes lack surface waves and a distinct $L_g$ phase. These events, which we interpret as having mantle source depths, do separate from the explosions on high-frequency $P/S$ discrimination plots.

**Key Words**: seismic discrimination, China

## OBJECTIVE

As part of the Comprehensive Test Ban Treaty (CTBT) research and development program, we have been evaluating regional seismic discriminants for central Asia, emphasizing western China. We have obtained waveforms recorded with the Chinese Digital Seismic Network (CDSN) station WMQ and the Kyrgyz Network (KNET) station AAK (Figure 1). Besides recording local and regional earthquakes, WMQ recorded several explosions in 1988 and 1989 from the former Soviet Union test site in Kazakhstan (KTS). AAK was installed in 1990, after testing ended at KTS, but the station has recorded regional seismicity and underground nuclear explosions from the Chinese test site at Lop Nor since 1991.

Our primary goal has been to evaluate many combinations of phases, frequency bands, and types of measurements for their potential as seismic discriminants. Hence, using seismograms from WMQ and AAK, we measured RMS, peak-to-peak, and peak-envelope amplitudes for the phases $P_n$, $P_g$, $S_n$, $L_g$, $L$ (Love waves), and $R$ (Rayleigh waves) over many frequency bands. We tested five general classes of seismic discriminants: (1) short-period phase ratios, such as $P_g$ (3–6 $Hz$) / $L_g$ (3–6 $Hz$) (both phases measured in the same frequency band); (2) short-period spectral ratios, such as $L_g$ (0.75–1.5 $Hz$) / $L_g$ (3–6 $Hz$); (3) short-period cross-spectral ratios, such as $P_g$ (0.75–1.5 $Hz$) / $L_g$ (3–6 $Hz$); (4) short-period to long-period ratios, such as $P_g$ (0.75–1.5 $Hz$) / $L$ (8–16 $s$); and (5) long-period Rayleigh-wave to Love-wave ratios, such as $R$ (8–16 $s$) / $L$ (8–16 $s$). We found that all five classes of these discriminants are useful for separating earthquakes from explosions in central Asia, provided the right combinations of frequency bands and phases are selected. For details that are not covered in this summary, *see Hartse et al.* (1996).

## REASEARCH ACCOMPLISHED

*Seismic Stations and Data*

We obtained all seismograms from the IRIS Data Management Center (DMC). WMQ (Figure 1) was upgraded to a CDSN station in 1986, and digital data is available from 1988 to the present. Digital data from KNET station AAK is available from 1990 to the present. For both stations, we requested data recorded with three-component, broadband (BH) seismometers (20 sps). For WMQ, instrument response is nearly flat to ground velocity between 0.03 and 4 Hz. For AAK, instrument response is nearly flat from 0.004 Hz to 6 Hz. We requested waveforms at both stations by using the United States Geologic Survey PDE catalogs maintained at the IRIS DMC as a guide. These are global catalogs, and for central Asia they include only those events with $m_b \approx 4.0$ and greater. We requested all PDE events between latitudes 55°N and 38°N and longitudes 100°E and 75°E (Figure 1). To request records from smaller events (down to $m_b \approx 2.5$), we used local Chinese catalogs, available for the 1970's and 1980's (Gao and Richards, 1994). With these "PRC" catalogs we were limited to data requests for the years 1988 and 1989 as WMQ data is not available prior to 1988.

Nuclear explosions from Lop Nor have been recorded at station AAK (about 1200 km west of the test site) since 1992. However, due to station down time, both Lop Nor explosions from 1994 were not recorded with the broadband components. Seismograms of only one Lop Nor nuclear test recorded at WMQ are available at the IRIS DMC. However, 17 nuclear explosions from KTS (≈ 950 km northwest of WMQ) were recorded in 1988 and 1989. We processed a total of 256 suspected earthquakes and 18 nuclear explosions recorded at WMQ. We are not certain that all PRC events are earthquakes. A few of these events could be chemical explosions from mines, but in this paper we treat all PRC events as earthquakes. Magnitudes ($m_b$) range between 2.5 and 6.1 for the earthquakes and between 4.5 and 6.1 for the explosions. The maximum event-station distance is 1205 km. For AAK, we processed 101

earthquakes and 5 nuclear explosions. Magnitudes range between 3.7 and 6.1 for the earthquakes and 5.0 and 6.5 for the explosions. The maximum event-station distance is 1704 km.

*Event Processing*

Event processing involved (1) converting SEED-format waveform data to SAC files, (2) picking body wave phases (when possible), (3) correcting records for instrument response (final units are ground velocity in $m/s$), (4) bandpass filtering, (5) making RMS, peak-to-peak, and peak-envelope amplitude measurements, (6) correcting for distance (path) effects, and (7) plotting phase ratios versus event magnitude to test discriminants. Measurements were made on vertical component seismograms, except for $L$, for which we rotated the horizontal components to obtain transverse record. When clearly visible, we hand picked body wave phases ($P_n$, $S_n$, $P_g$, and $L_g$) from the three-component BH records. We estimated velocities for the body wave phases from traveltime - distance plots, and then defined "data window" velocities that surround the body wave velocities. For surface wave processing, we visually examined many Love-wave and Rayleigh-wave arrivals, and then selected velocities that defined measurement windows surrounding the peak-to-peak maximums of $L$ and $R$. For each phase measurement we also made a pre-$P_n$ noise measurement.

Figure 2 shows sample waveforms of the Lop Nor nuclear explosion recorded at WMQ (BHZ component) and a nearby earthquake. The unfiltered (*top*) traces show the first arrival ($P_n$), and the two lower seismograms show bandpass-filtered seismograms with $P_g$ and $L_g$ measurement windows marked. For each window, we measured ($\log_{10}$) RMS amplitude, the maximum peak-to-peak amplitude, and the peak-envelope amplitude.

We computed distance corrections by linear regression of earthquake ratios on the logarithm (base 10) of distance, and applied the corrections to both earthquake and explosion ratios. For each regression we used earthquake ratios formed with signal measurements at least 10 times greater than pre-$P_n$ noise levels. When actually applying the regression results and forming the discrimination plots, we used ratios of earthquakes and explosions formed with signal measurements at least twice the pre-$P_n$ noise level. We used the reported PDE $m_b$ magnitudes and, for the small earthquakes, the Chinese local magnitudes ($M_L$).

*Discrimination*

We tested many combinations of phases and frequency bands as event discriminants. Here, we qualitatively class discriminants as good, fair, or poor. We will report on quantitative discriminant performance in a later paper. Below, are some examples of discrimination ratios that separate earthquakes from explosions, and also some examples that are known to work in the western United States, but are poor discriminants in central Asia. All ratios have been corrected for a distance effect, as described in the previous section, and all measurements used to form ratios have signal that is at least twice the pre-$P_n$ noise level.

*Short-Period Discriminants*

*Phase ratios.* Many short-period regional discriminants that exploit a $P/S$ ratio have been discussed in the literature (*cf.* Pomeroy *et al.*, 1982). Figure 3 shows examples of the $P_g/L_g$ ratio versus $m_b$. We show two bands with center frequencies of 1.125 and 4.5 Hz. The 0.75-1.5 Hz $P_g/L_g$ ratio fails to separate the explosions and earthquakes. However, as frequency increases, the explosion and earthquake separation increases substantially. For frequency bands above 3 to 4 Hz, the explosions and earthquakes can be separated with $P_g/L_g$, $P_n/L_g$, and $P_n/S_n$ ratios.

These high-frequency ($f > \approx 4$ Hz) $P/S$ ratios work for northwest-southeast paths from KTS to WMQ, a distance of about 950 km. Considering the similarity of the source-area geology at KTS and Lop Nor (*i.e.* hard rock sites, Matzko (1994)), we anticipate that these ratios will work for reversed paths from the Lop Nor area into Kazakhstan. The primary drawback of this discriminant is that it depends on high frequencies for both $P$ and $S$. For explosions, $S_n$ and $L_g$ are low-amplitude phases, and for passbands above $\approx 4$ Hz, an $m_b$ of nearly 5.0 is required before signal exceeds noise at recording distances of $\approx 1000$ km.

*Spectral Ratios.* Spectral discriminants have been successfully applied to relatively small events ($3.0 < m_b < 4.8$) from the western United States. Taylor *et al.* (1988) used the $L_g\,(1\text{–}2\,Hz)$ / $L_g\,(6\text{–}8\,Hz)$ ratio, Bennett and Murphy (1986) used the $L_g\,(0.5\text{–}1\,Hz)$ / $L_g\,(2\text{–}4\,Hz)$ ratio, Hartse *et al.* (1995) used the coda $(0.5\text{–}1\,Hz)$ / $(2\text{–}4\,Hz)$ ratio, and Walter *et al.* (1995) used $P_n$, $P_g$, $L_g$ and $L_g$ coda ratios to separate nuclear explosions from earthquakes. Figure 4 shows that some spectral discriminants do separate earthquakes and explosions in central Asia, but the $L_g$ spectral discriminant does not. The western U.S. studies generally examined small explosions ($m_b < 4.8$) that were detonated above the water table. Most explosions from Lop Nor are thought to be detonated below the water table (Matzko, 1994). As discussed by Taylor and Denny (1991), Patton and Taylor (1995), and Walter *et al.* (1995), the amount of gas-filled porosity near the explosion appears to control the performance of the $L_g$ spectral-ratio discriminant. In the western United States, $L_g$-waves from explosions are deficient in high frequency energy relative to earthquakes. For the KTS and Lop Nor explosions, the $P_n$, $P_g$, and $S_n$ phases have a high-frequency enhancement relative to regional earthquakes of similar magnitudes.

The $P_n$, $P_g$, and $S_n$ ratios for the 3-6/0.75-1.5 Hz bands all separate explosions from earthquakes. Taylor and Denny (1991) and Taylor and Marshall (1991) have noted that a high-frequency to low-frequency ratio of $P$ waves recorded at teleseismic distances separates Kazakh nuclear explosions from Asian earthquakes. Arora and Basu (1984) noted a similar relationship for Lop Nor explosions and western China earthquakes recorded in southern India. Figure 4 shows that these relationships can also be observed at regional distances, at least for explosions down to $m_b \approx 4.5$.

*Cross-Spectral Ratios.* The spectral ratios of Figure 4 imply that the $P$ energy generated by Lop Nor and KTS explosions is rich in high frequencies ($f > 4$ Hz) relative to regional earthquakes. At the same time Figure 2 suggests that the explosions have relatively less $L_g$ energy than the earthquakes. Hence, a $P$ phase with $f > \approx 4$ Hz in ratio with an $S$ phase of any short-period band should be a good discriminant.

Figure 5 shows examples of the cross-spectral discriminants that we tested. The high-frequency $P$ to low-frequency $S$ ratios have an important advantage over the high-frequency phase ratios (Figure 3). Because event separation can be obtained using $S$ in frequency bands near 1 Hz, the lower magnitude explosions, which have $S_n$ and $L_g$ energy levels above background noise, can be included in the discrimination plots. Hence, these cross-spectral ratio discriminants can be applied to smaller explosions and out to greater distances than the high-frequency phase ratios. For example, the cross-spectral plot of Figure 5a includes an $m_b = 4.6$ KTS explosion that was dropped from the 3-6 Hz $P_g/L_g$ phase-ratio plot of Figure 3a due to a low signal-to-noise ratio.

*Short-Period/Long-Period Ratios.* We tested $P/R$ and $P/L$ ratios for several bands. As our study of central Asia progresses, we will develop regional $m_b$ and $M_S$ magnitude scales, enabling us to present the $P_n/R$ ratio in its more common form, the $m_b : M_s$ discriminant. The $m_b : M_s$ discriminant has been successfully applied at regional distances in the western United States by Taylor *et al.* (1989). We measured peak-to-peak and peak-envelope velocity

amplitudes from broadband records to test this discriminant. Peak-envelope measurements show less scatter than the peak-to-peak measurements.

Figure 6 shows examples of short-period / long-period discrimination plots. The $P_n$ $(0.75–1.5\,Hz)$ / $R$ $(8–16\,s)$ ratio, provides good separation between earthquakes and explosions. As in the case of phase ratios and cross-spectral ratios, raising the $P_n$ band to 3-6 Hz improves event separation when ratios are formed with $R$. We tested a $P_n$ $(0.75–1.5\,Hz)$ / $L$ $(8–16\,s)$ ratio, which separates explosions and earthquakes, but requires a large explosion before $L$ can be measured above the noise. Although we do not show examples here, the $P_g/R$, $P_n/L$, and $P_g/L$ ratios are all improved by measuring higher frequency body waves. The primary drawback of the short-period / long-period discriminant is the weak surface waves generated by the explosions. Most explosions we processed are recorded at more than 950 km. With closer recording distances and signal enhancement through array processing, the short-period / long-period discriminants may become more useful for separating smaller events.

*Long-Period Ratios.* We tested long-period $R/L$ discriminants, and found that the 6-12 s and 8-16 s periods show the best separation and least scatter. The $R/L$ discriminant was mentioned by Pomeroy *et al.* (1982), but has not been widely tested or applied. The primary drawback is that the weak $L$ of the explosions often fail to exceed noise levels. The Kazakh explosions had to be large ($m_b > 5.0$) to generate $L$ that was above the noise at WMQ (Figure 8d).

The PDE catalog lists the depths of the six Pamir events as 33 km, but we suspect that at least four of these earthquakes are deep (mantle source). We identify these events with a special symbol on the discrimination plots shown in Figures 3-6.

## RECOMMENDATIONS AND FUTURE PLANS

We have measured noise and phase amplitudes of over 250 earthquakes and 18 underground nuclear explosions recorded at the broadband, digital station WMQ in western China and over 100 earthquakes and 5 nuclear explosions at station AAK in Kyrgyzstan. Event magnitudes ($m_b$) range between 2.5 and 6.5 and maximum event-station distance is about 1700 km. Using these measurements we formed phase, spectral, cross-spectral, short-period/long-period, and long-period ratios to test many possible event discriminants. All ratios were corrected for distance effects before plotting ratio-versus-magnitude discrimination plots.

The most consistent discriminants for separating earthquakes from explosions are a high-frequency ($f \gtrsim 4\,Hz$) $P/S$ ratio versus $m_b$ and a short-period $P$ ($f \gtrsim 1\,Hz$) to long-period Rayleigh-wave ($0.05 < f < 0.1$) ratio versus $m_b$. The short-period $P/S$ ratio was even successful at separating several apparently deep earthquakes from the North Pamir region of far western China, which merge with explosions on spectral and cross-spectral discrimination plots.

$P_n$, $P_g$, and $S_n$ spectral ratios ($\approx 3–6\,Hz$ / $0.75–1.5\,Hz$) and $P$ ($\approx 3–6\,Hz$) / $S$ ($\approx 0.75–1.5\,Hz$) cross-spectral ratios also separate most earthquakes from the explosions. The KTS explosions separate from earthquakes when an $R/L$ ratio is formed. However, the large Lop Nor explosions do not separate from the earthquakes when the $R/L$ ratio is formed, indicating strong tectonic release may be associated with explosions at the Lop Nor test site.

We plan to continue this study by collecting and analyzing waveform data from other Asian seismic stations. Future studies will include detailed analysis of the suspected deep Pamir earthquakes, development of regional magnitude scales, and efforts to incorporate small ($2.0 < m_b < 3.5$) chemical explosions into our event discrimination plots. Because we evaluate several different discriminants, we will develop multivariate techniques that combine

measurements and quantitatively assess discrimination performance.

## Acknowledgements

Brian Stump provided a thoughtful review of this manuscript. We thank the staff at the IRIS Data Management Center for prompt replies to our data requests. The GMT mapping software (Wessel and Smith, 1991) was used to construct Figure 1. This work is in support of the DOE Comprehensive Test Ban Treaty Research and Development Program, ST482A, and was performed at Los Alamos National Lab under the auspices of the United States Department of Energy, Contract Number W-7405-ENG-36.

## References

Arora, S. K. and T. K. Basu (1984). A source discrimination study of a Chinese seismic event of May 4, 1983, *Tectonophysics*, **109**, 241-251.

Bennett, T. and J. Murphy (1986). Analysis of seismic discrimination using regional data from western United States events, *Bull. Seis. Soc. Am.*, **76**, 1069-1086.

Gao, L. and P. G. Richards (1994). Studies of earthquakes on and near the Lop Nor, China, nuclear test site, *Proceedings of the 16th Annual DARPA/AF Seismic Research Symposium*, 106-112.

Hartse, H. E., W. S. Phillips, M. C. Fehler, and L. S. House (1995). Single-station spectral discrimination using coda waves,, *Bull. Seis. Soc. Am.*, **85**, 1464-1474.

Hartse, H. E., S. R. Taylor, W. S. Phillips, and G. E. Randall (1996). Single-station spectral discrimination using coda waves,, *Bull. Seis. Soc. Am.*, **86**, submitted.

Matzko, J. R. (1994). Geology of the Chinese nuclear test site near Lop Nor, Xinjiang Uygur Autonomous Region, China, *Engineering Geololgy*, **36**, 173-181.

Patton, H. J. and S. R. Taylor (1995). Analysis of *Lg* spectral ratios from NTS explosions: Implications for the source mechanism of spall and the generation of *Lg* waves, *Bull. Seism. Soc. Am.*, **85**, 220-236.

Pomeroy, P. W., J. B. Best, and T. V. McEvilly (1982). Test ban treaty verification with regional data - a review, *Bull. Seis. Soc. Am.*, **72**, S89-S129.

Taylor, S. R. and M. D. Denny (1991). An analysis of spectral differences between Nevada Test Site and Shagan River nuclear explosions, *J. Geophys. Res.*, **96**, 6237-6245.

Taylor, S. R. and P. D. Marshall (1991). Spectral discrimination between Soviet explosions and earthquakes using short-period array data, *Geophy. J. Int.*, **106**, 265-273.

Taylor, S. R., N. W. Sherman, and M. D. Denny (1988). Spectral discrimination between NTS explosions and western United States earthquakes at regional distances, *Bull. Seis. Soc. Am.*, **78**, 1563-1579.

Taylor, S. R., M. D. Denny, E. S. Vergino, and R. E. Glaser (1989). Regional discrimination between NTS explosions and western U.S. earthquakes, *Bull. Seis. Soc. Am.*, **79**, 1142-1176.

Walter, W. R., K. M. Mayeda, and H. J. Patton (1995). Phase and spectral ratio discrimination between NTS earthquakes and explosions. Part I: Empirical Observations, *Bull. Seism. Soc. Am.*, **85**, 1050-1067.

Wessel, P. and W. H. F. Smith (1991). Free software helps map and display data, *EOS Trans. AGU*, **72**, 441.

**Figure 1.** Study area map showing, shaded topography, nuclear explosion and test site locations, natural seismicity, and seismic stations. We used seismic data recorded at stations WMQ and AAK in this study.

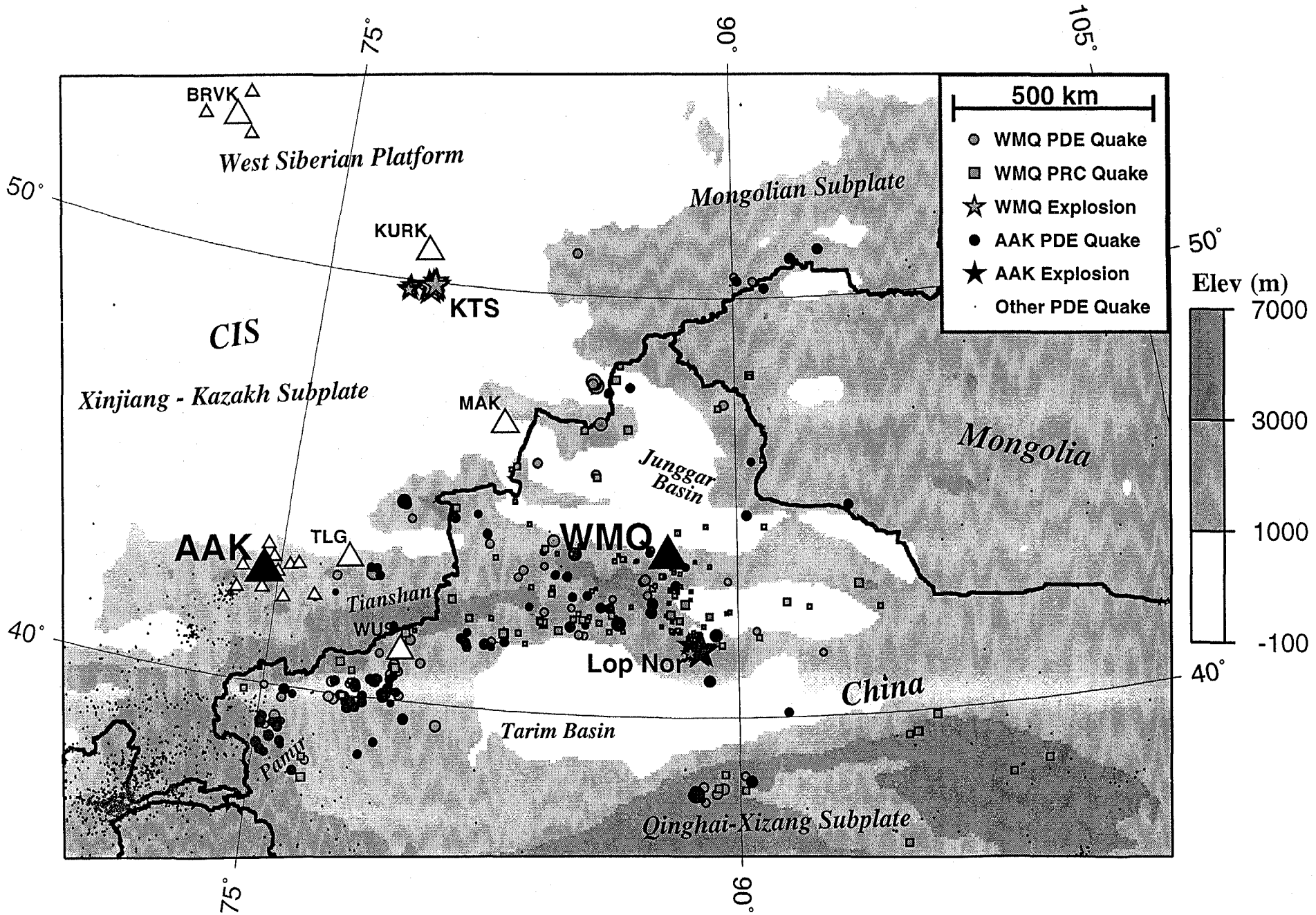

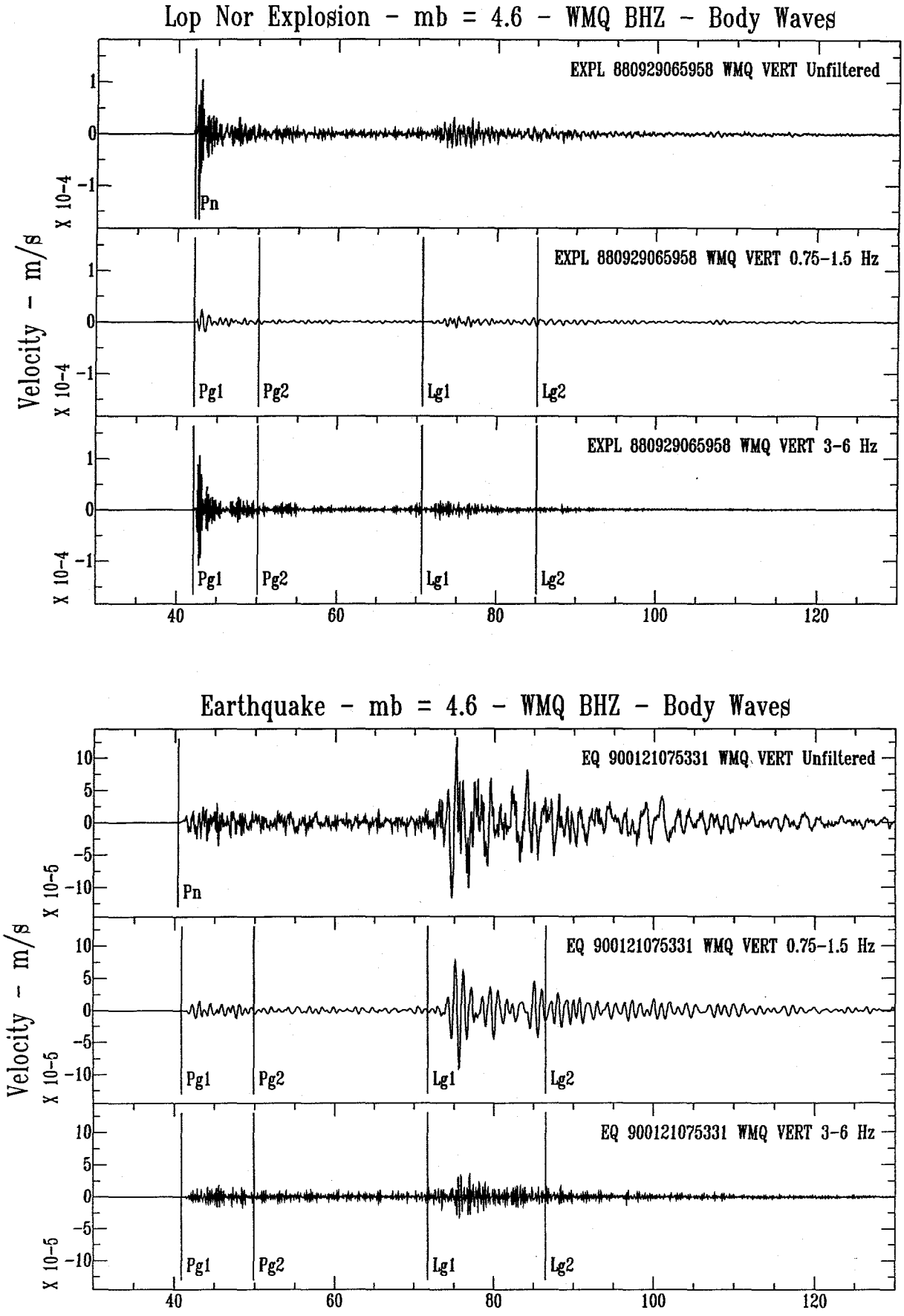


**Figure 2.** Sample waveforms from a Lop Nor nuclear explosion (top) and a nearby earthquake recorded at station WMQ. Event-station distance for both events is about 250 km. Note that $P$ for the explosion is enhanced in 3-6 Hz energy relative to the earthquake. $L_g$ for the explosion is deficient in frequencies above $\approx 1\,Hz$ relative to the earthquake.

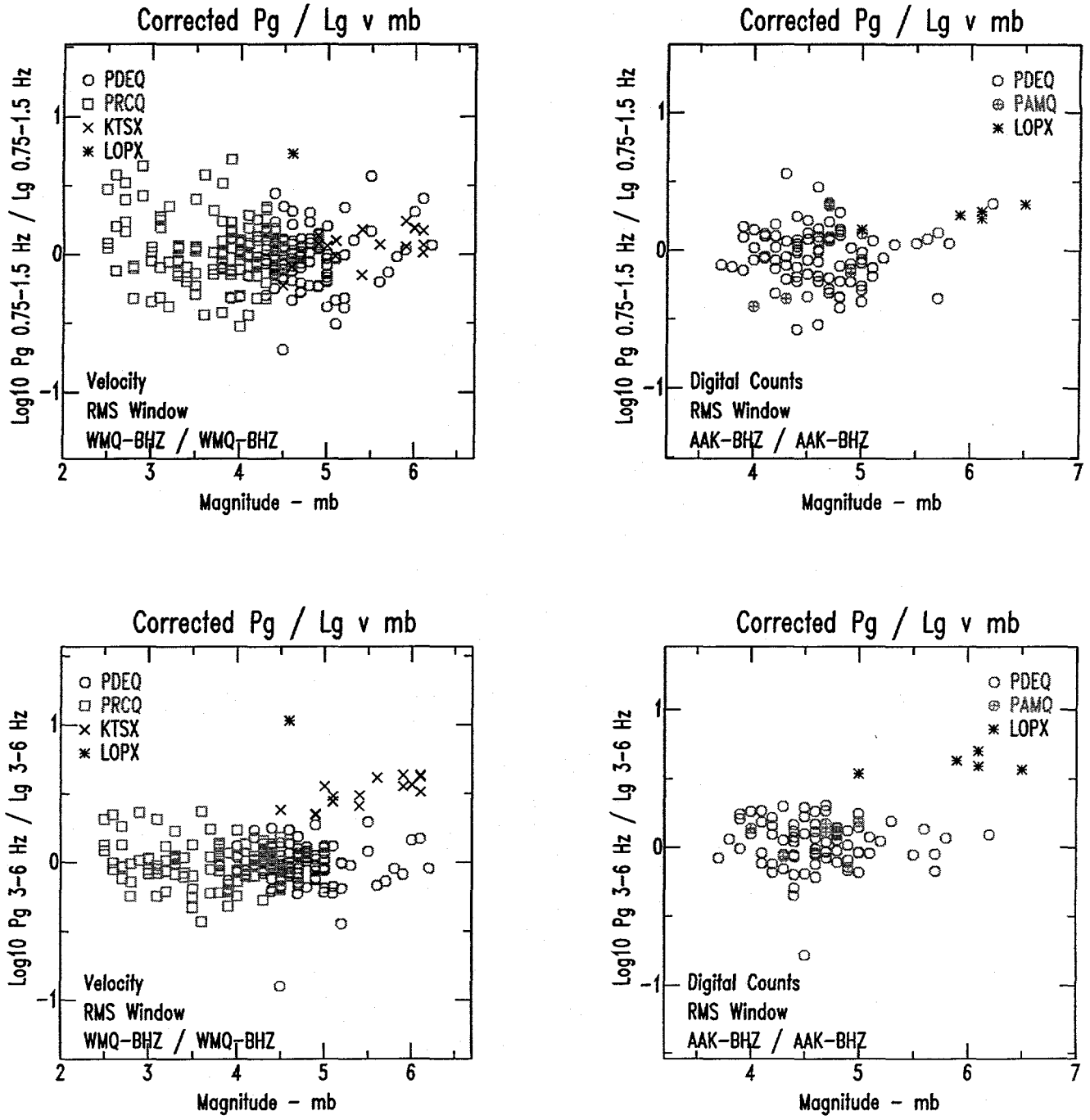


**Figure 3.** Phase ratio $P_g/L_g$ discrimination plots for stations WMQ (left) and AAK. Center frequencies are 1.125 Hz and 4.5 Hz. As frequency increases, separation between earthquakes and explosions also increases.

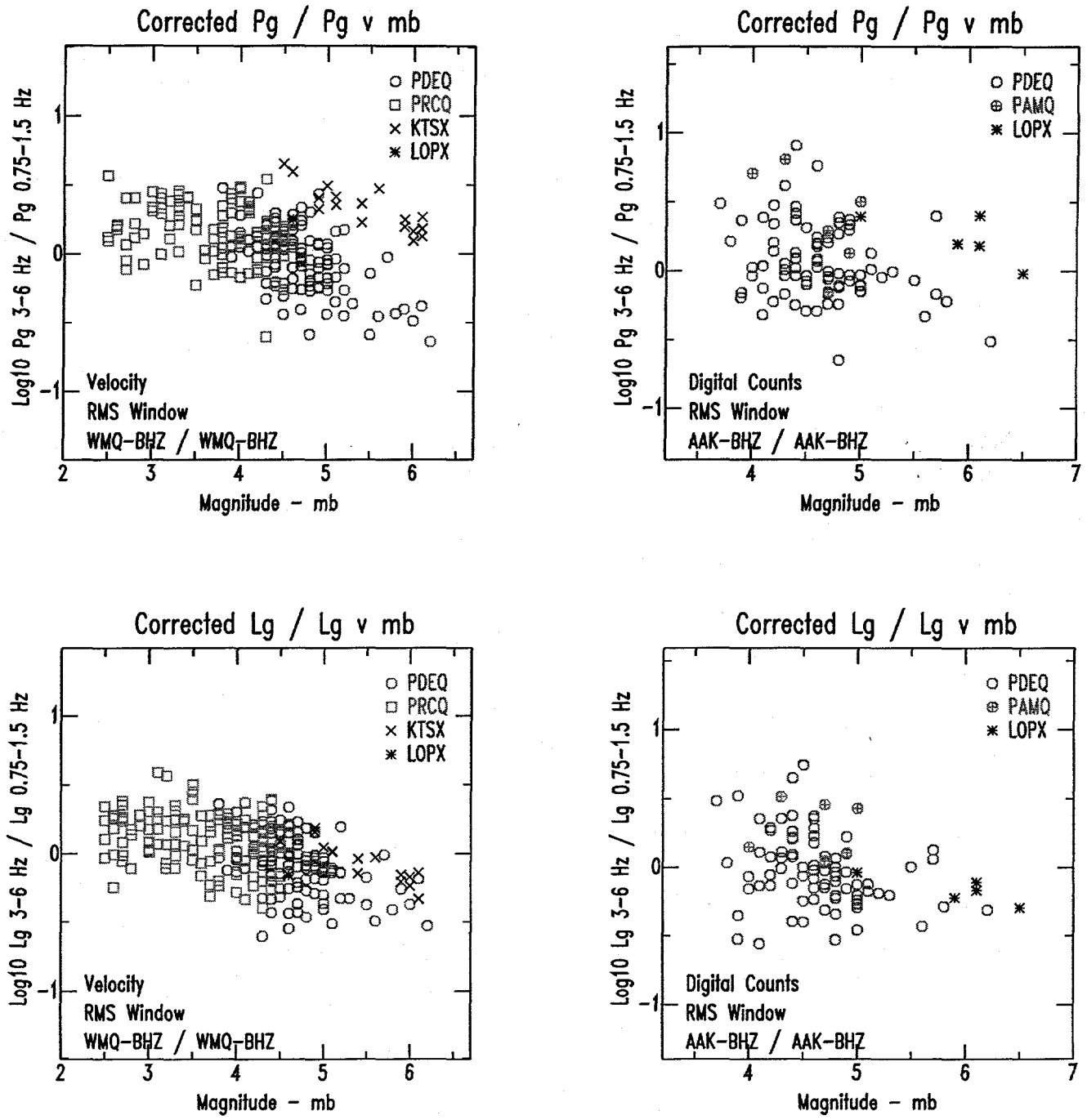


**Figure 4.** Spectral ratio discrimination plots for stations WMQ (left) and AAK. In contrast to the western United States, the $L_g$ spectral ratio (bottom) performs poorly in central Asia. Some of the suspected sub-crustal earthquakes from the Pamir uplift (PAMQ) merge with the explosions at AAK (top left).

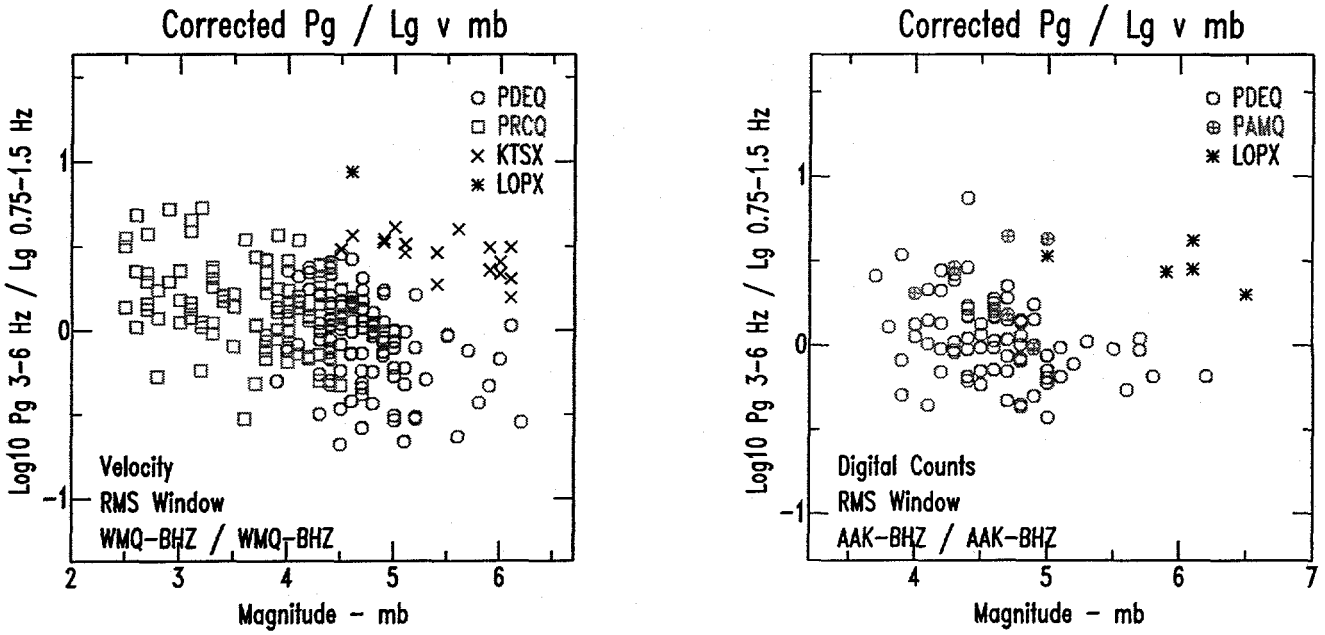


**Figure 5.** Cross-spectral ratio discrimination plots for stations WMQ (left) and AAK. Using $L_g$ measured at around 1 *Hz* allows us to evaluate smaller explosions compared to using $L_g$ measured at around 4 *Hz* (see Figure 3). Some of the suspected sub-crustal earthquakes from the Pamir uplift (PAMQ) merge with the explosions at AAK (left).

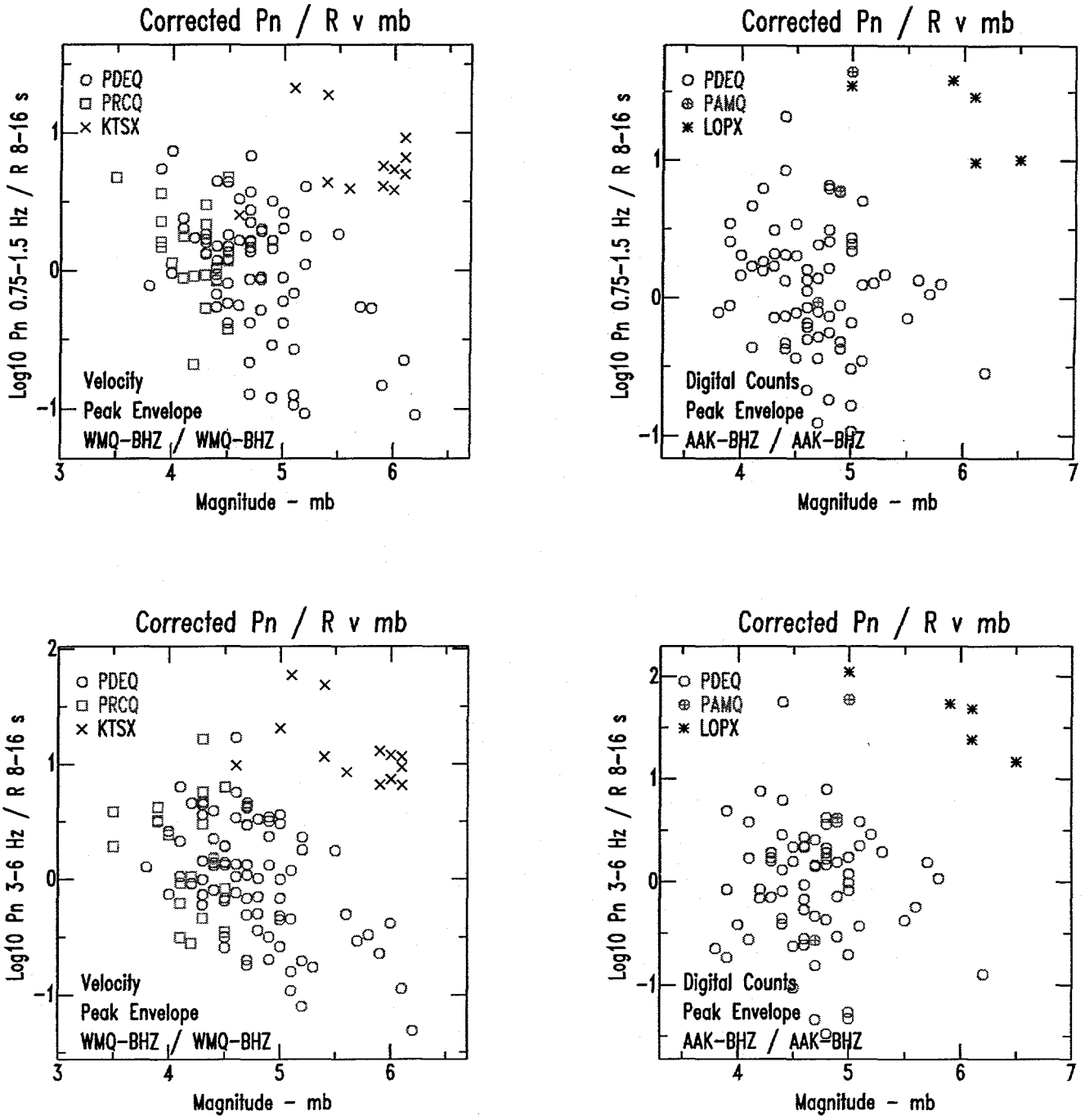


**Figure 6.** Short-period / long-period discrimination plots for stations WMQ (left) and AAK. Here we show $P_n$ in ratio with $R$, but $P_n$ in ratio with $L$ also performs well. As $P_n$ frequency increases, separation increases.